Focusing effect measurements of artificial dielectric multilayer lens with metal rectangular chips for terahertz wave band

Yuki Takebayashi, Takuya Konno, Shouhei Shimada, Fumiaki Miyamaru, John C. Young, Hideaki Kitahara, Keisuke Takano, Masanori Hang et al.

Applied Physics A
Materials Science & Processing

ISSN 0947-8396

Appl. Phys. A
DOI 10.1007/s00339-013-8074-8

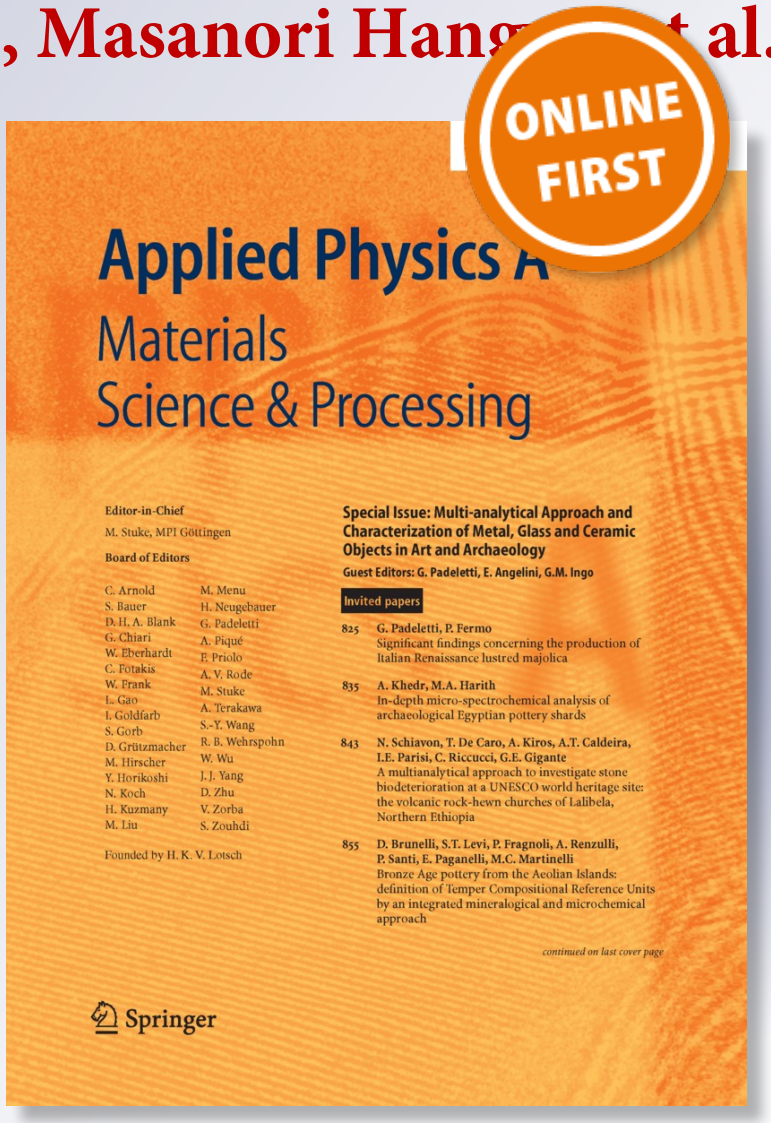

Springer

Appl. Phys. A
DOI 10.1007/s00339-013-8074-8

Applied Physics A
Materials Science & Processing

Focusing effect measurements of artificial dielectric multilayer lens with metal rectangular chips for terahertz wave band

Yuki Takebayashi · Takuya Konno · Shouhei Shimada · Fumiaki Miyamaru · John C. Young · Hideaki Kitahara · Keisuke Takano · Masanori Hangyo · Takehito Suzuki

Received: 10 October 2013 / Accepted: 13 October 2013

Abstract This paper presents the design and fabrication of an artificial multilayer lens comprising ten layers of metal rectangular chips on a cyclo olefin polymer, which has low loss in the terahertz band. Measurements of the focusing effect are also presented. The focusing effect is produced by the rectangular metallic chips which act as an electrical dipole. Simulations are performed using ANSYS HFSS. The lenses are fabricated by laser processing or semiconductor etching. The focusing effect is confirmed by measurement using terahertz near-field microscopy, although some discrepancies are observed between the simulated and measured results.

1 Introduction

Due to the increasing use of the terahertz wave band, the need for high-performance optical devices in the terahertz band is expanding. However, the realization of a desired refractive index using naturally-occurring materials can be quite difficult. When a material is directly used to construct an optical device, the material properties determine the device's optical characteristics. High density polymer lenses, Tsurupica lenses, and silicon lenses with refractive indices of 1.52, 1.56, and 3.41, respectively, are typical terahertz band lenses. Microwave-band lenses composed of electromagnetic metamaterials were proposed in [1–5].

For the terahertz-band, a metamaterial absorber is presented in [6–9], a metamaterial with an unnaturally high refractive index is presented in [10], an antireflection coating is presented in [11], and flat metamaterial lenses in [12–16]. The work in [17] presented an artificial dielectric lens with metallic rectangular chips for the terahertz band. The fabrication of terahertz electromagnetic metamaterials by laser processing, metallic processing, semiconductor etching and chemical reduction [18,19] is relatively easy compared with fabrication of metamaterials in the optical range since the dimensions of the unit element are on the order of microns. Furthermore, the unit cell of the electromagnetic metamaterial, which controls the refractive index, is of prime importance with respect to design flexibility and cost performance.

This paper presents a terahertz-band artificial multilayer lens with ten layers of metal rectangular chips [17] on a cyclo olefin polymer, which has low loss in terahertz band. In this metallic lens, each of the rectangular metallic chips acts as an electrical dipole and the behavior is similar to a dielectric material. The rectangular chips with macroscopic dimensions are used for the artificial dielectric lens instead of the molecules and atoms with microscopic dimensions for the dielectric lens. This artificial dielectric lens does not work by taking advantage of resonance effect [1,20], so the lens is not narrow band. The work in [17] presented the operational principle of this artificial dielectric lens and the determination of the performance. The artificial lens is depicted in Fig. 1.

Y. Takebayashi · T. Konno · T. Suzuki (✉)
Department of Electrical and Electronic Engineering, Ibaraki University, 4-12-1 Nakanarusawa, Hitachi, Ibaraki 316-8511, Japan
e-mail: takehito@mx.ibaraki.ac.jp

S. Shimada · F. Miyamaru
Department of Physics, Shinshu University, 3-1-1 Asahi, Matsumoto, Nagano 390-8621, Japan

J. C. Young
Electrical and Computer Engineering, University of Kentucky, Lexington, KY 40506-0046, USA

H. Kitahara · K. Takano · M. Hangyo
Institute of Laser Engineering, Osaka University, 2-6 Yamadaoka, Suita, Osaka 565-0871, Japan

Published online: 15 November 2013

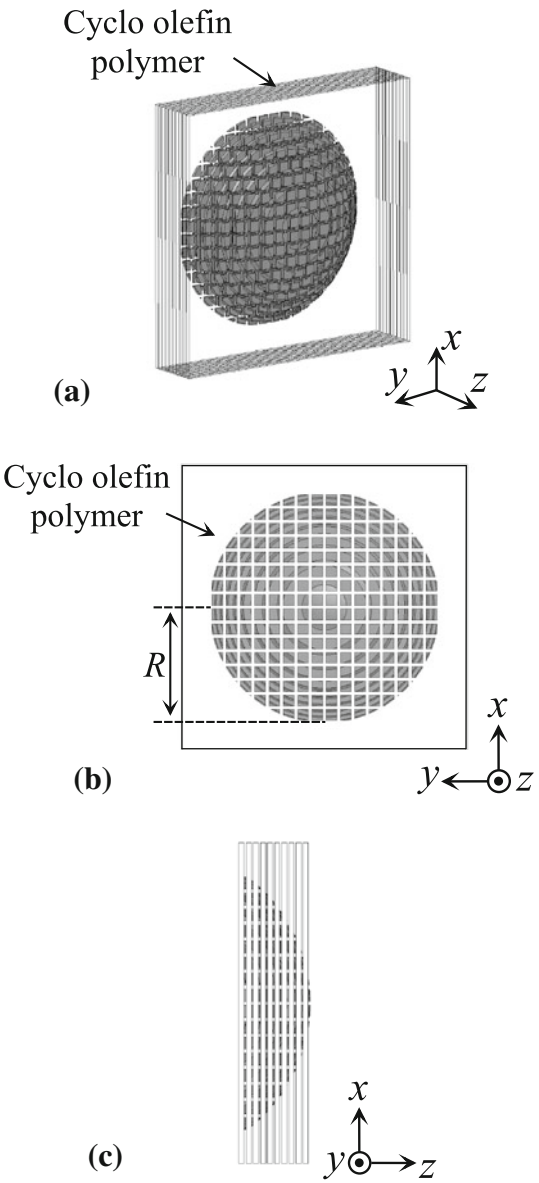

Fig. 1 Lens with metal rectangular chips on cyclo olefin polymer. **a** Bird's-eye view, **b** top view, **c** side view

The benefit of this lens is that the refractive index can be spatially controlled by the unit parameters of the rectangular chips. Furthermore, measurements of the focusing effect are also presented. The focusing effect is produced by the rectangular metallic chips that act as an electrical dipole. Two types of lens are fabricated as shown in Fig. 2. One lens is fabricated by laser processing and has a chrome buffer layer. The other lens is fabricated by semiconductor etching and does not have a buffer layer. The focusing effects are measured by terahertz near-field microscopy [21]. Section 2 explains the lens parameters. Section 3 presents the full wave analysis model with and without the buffer chrome layer. Section 4 discusses the measurement results.

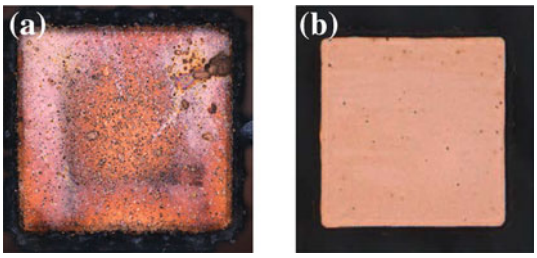

Fig. 2 Fabrication method. **a** Laser process, **b** etching process

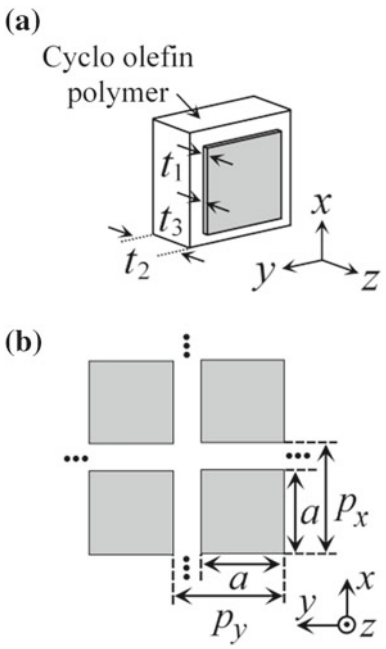

Fig. 3 Unit cell models. **a** Bird's-eye view, **b** top view

Table 1 Parameters for lens with chrome buffer layer

a	75 μm
p_x	100 μm
p_y	100 μm
t_1	0.35 μm
t_2	100 μm
t_3	10 nm
R	2.2 mm

Table 2 Parameters for lens without chrome buffer layer

a	120 μm
p_x	160 μm
p_y	160 μm
t_1	0.5 μm
t_2	50 μm
R	3.0 mm

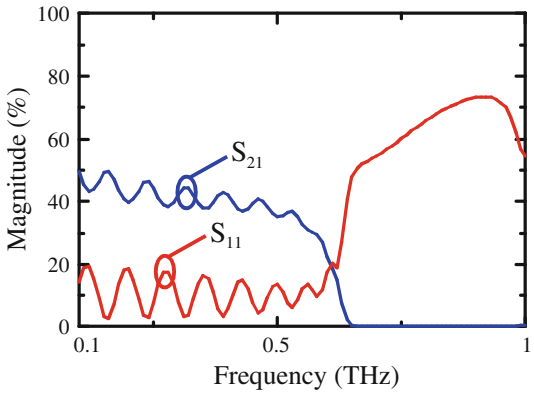

Fig. 4 Transmission loss with buffer layer

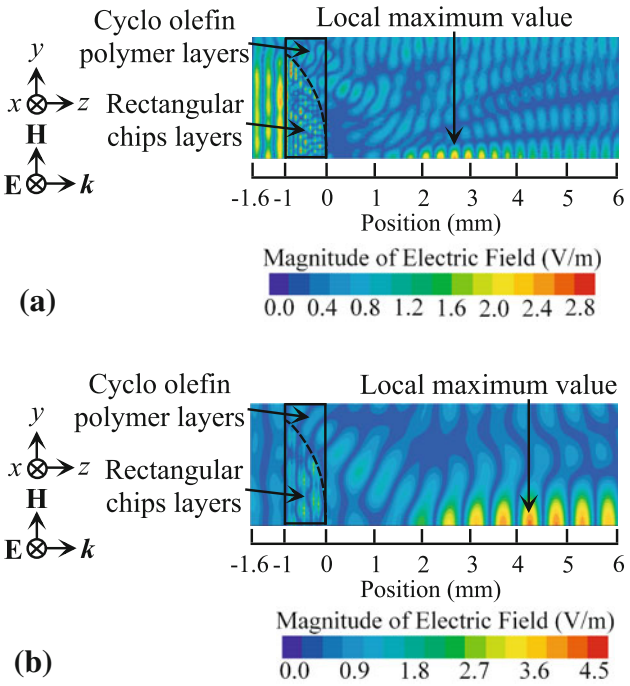

Fig. 5 Full wave analysis results for lens with buffer layer at (**a**) 0.63 and (**b**) 0.30 THz

2 Lens parameters

Figure 3 depicts the unit cell model. The rectangular chips are fabricated on a cyclo olefin polymer which has a refractive index of 1.53 and has low loss in the terahertz band. Table 1 shows the parameters of the lens with the chrome buffer layer. The chrome layer has a thickness of 10 nm, which produces losses, and is used as buffer layer. The lens with the chrome buffer layer is fabricated by laser processing. The laser process can realize the microfabrication, but it partially sears the metal. Table 2 shows the parameters of the lens without the chrome buffer layer. The lens without the chrome buffer layer is fabricated by semiconducting etching. Both lenses have ten layers of chips. The number of chips is

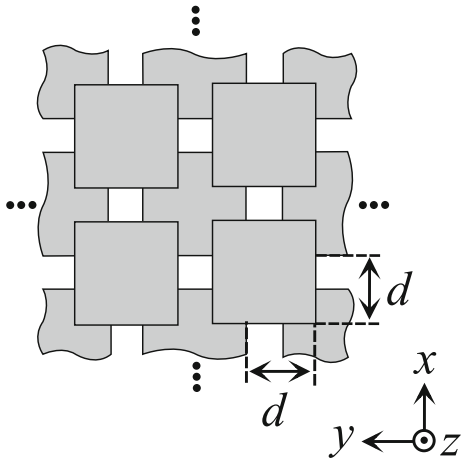

Fig. 6 Configuration with lamination errors

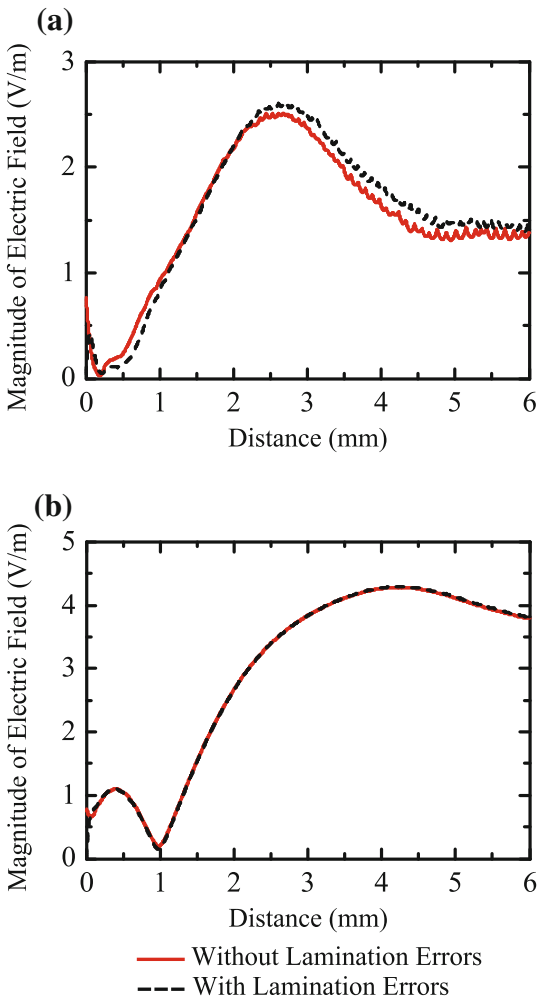

Fig. 7 Full wave analysis results that include lamination error for lens with buffer layer at (**a**) 0.63 and (**b**) 0.30 THz

different for each layer, and the number of chips decreases along the top of the lens. The dimensions of all chips are the same in all layers. The etching process can be used to fabri-

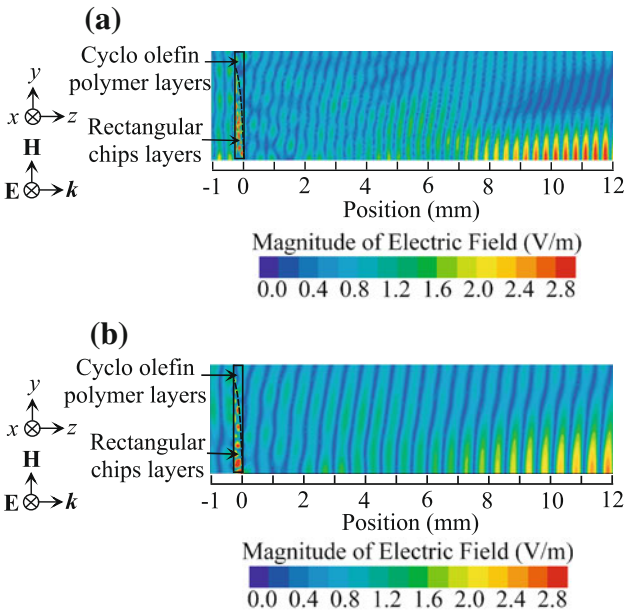

Fig. 8 Full wave analysis results for lens without buffer layer at (**a**) 0.48 and (**b**) 0.30 THz

cate a large area in one process, but it cannot realize smaller lens features than the laser process.

3 Loss of buffer layer

Low electrical conductivity results in relatively high conductor loss, which leads to the transmission loss. Figure 4 shows the analysis result of the buffer layer loss with ten layers. The lens parameter are listed in Table 1. The periodic boundary walls model is used to analyze the reflection characteristics S_{11} and transmission characteristics S_{21}. It is confirmed that a portion of the incident power is lost due to conductor loss.

4 Full wave analysis results

4.1 Full wave analysis results with chrome buffer layer

The full wave analysis results are obtained by ANSYS HFSS, where the incident electric field is 1 V/m. Only one quarter of the full model is analyzed using image theory [22]. Figure 5a shows the full wave analysis results with chrome buffer layer at 0.63 THz and Fig. 5b shows the results for 0.30 THz. The loss of the cyclo olefin polymer is not considered in the full wave analysis to reduce computation time and because the loss is expected to be low. The local maximum value of the electric field magnitude is 2.5 times that of the incident wave at 2.59 mm ($5.44\lambda_0$) for 0.63 THz. The local maximum

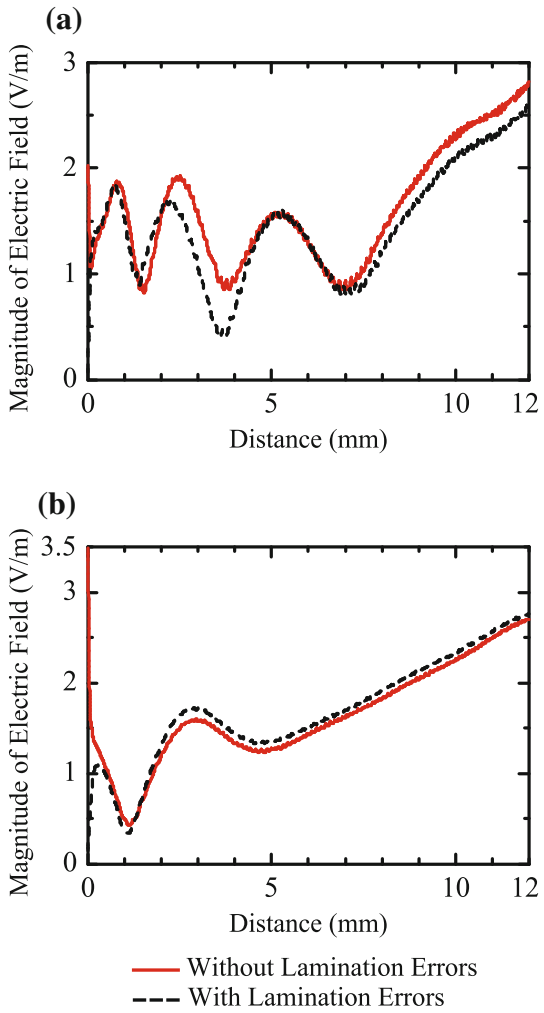

Fig. 9 Full wave analysis results that include lamination error for lens without buffer layer at (**a**) 0.48 and (**b**) 0.30 THz

value of the electric field magnitude is 4.3 times that of the incident wave at 4.16 mm ($4.16\lambda_0$) for 0.30 THz.

Figure 6 shows the configuration with the lamination errors d. Figure 7 shows the results taking the lamination errors with d = 50 into account. The red and black lines respectively show the results with lamination errors and without lamination errors. The focusing effects are not influenced much by the lamination errors at either 0.63 THz or 0.30 THz.

4.2 Full wave analysis results without buffer layer

Figure 8a and b shows the full wave analysis results without buffer layer for 0.48 and 0.30 THz respectively. Since the full 10 layer model is computationally huge, to reduce computation time, the analysis model is taken to be a 5 layer model with the same curvature radius as the fabricated model. In addition, the analysis does not include the loss in cyclo olefin polymer. The value of the electric field magnitude is 2.3 times

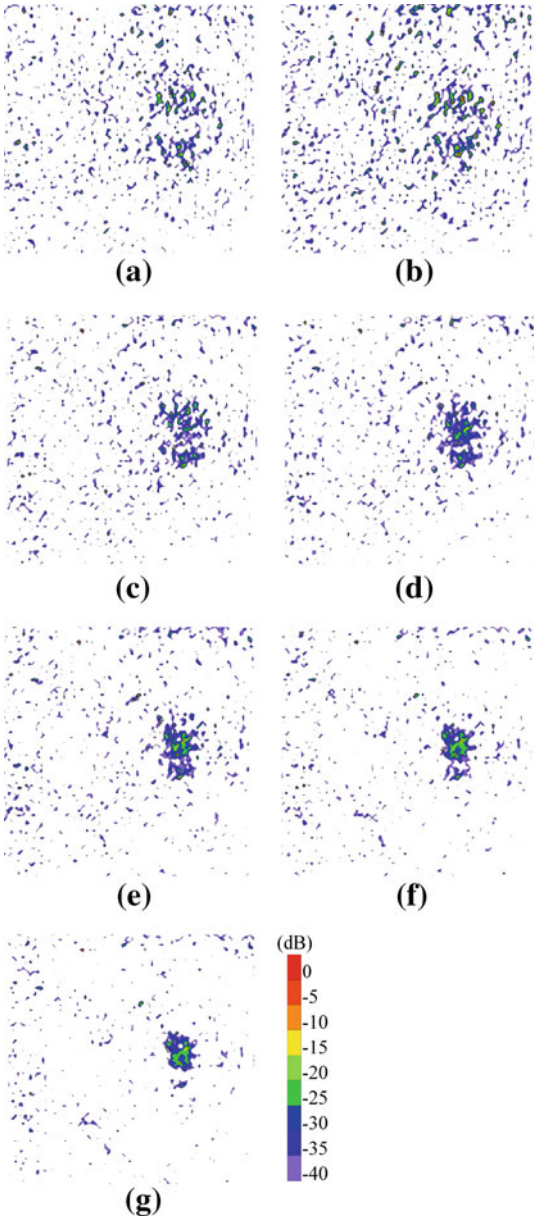

Fig. 10 Measurement results for aperture distribution of electric field through lens with buffer layer at 0.63 THz. (**a**) 1.23, (**b**) 1.73, (**c**) 2.23, (**d**) 2.73, (**e**) 3.23, (**f**) 3.73 and (**g**) 4.23 mm

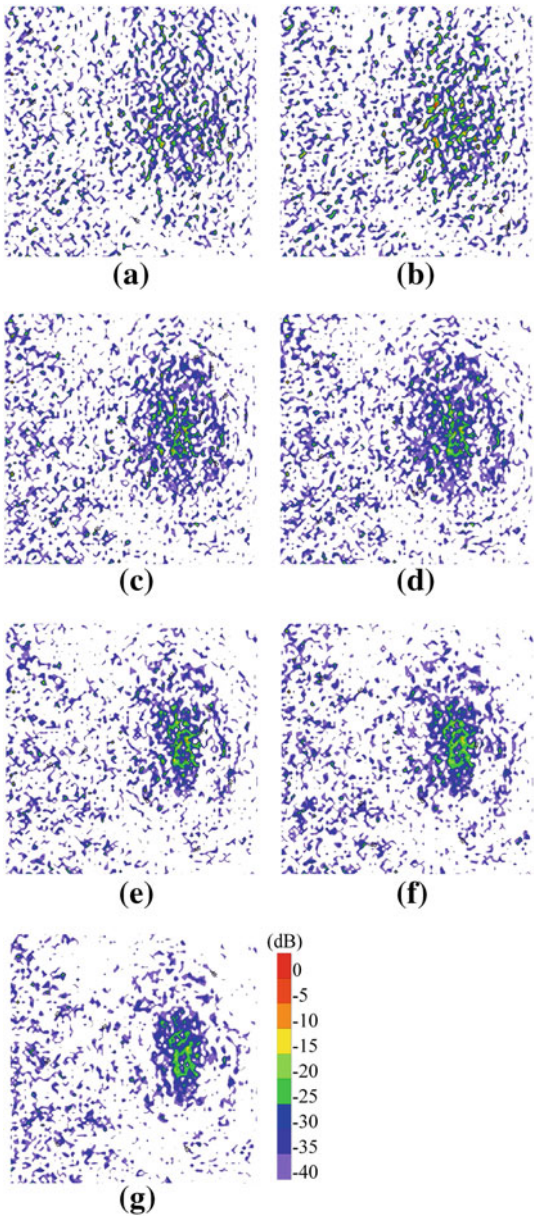

Fig. 11 Measurement results for aperture distribution of electric field through lens with buffer layer at 0.30 THz. (**a**) 1.23, (**b**) 1.73, (**c**) 2.23, (**d**) 2.73, (**e**) 3.23, (**f**) 3.73 and (**g**) 4.23

that of the incident wave at 9.85 mm ($15.6\lambda_0$) for 0.48 THz. The value of the electric field magnitude is 2.2 times that of the incident wave at 9.77 mm ($9.78\lambda_0$) for 0.30 THz. Figure 9 shows the results that include the lamination errors with $d = 80$. The red and black lines respectively show the results with lamination errors and without lamination errors. Again, the focusing effects are not influenced much by the lamination errors at either 0.48 THz or 0.30 THz. However, the lamination errors seem to have more influence for the lens without the buffer layer than for the lens with the buffer layer.

5 Measurement results

5.1 Measurement result for lens with chrome buffer layer

Figure 10 shows the measurement results for 0.63 THz and Fig. 11 shows the results for 0.30 THz. The measurements are performed using terahertz near-field microscopy [21]. The detection technique is electric optical detection using EO crystal. The diameter of incident beam size is 1.5 mm. The bandwidth is below 2.0 THz, and the amplitude is expressed using dB scale. The focusing effect increases from 1.23 to

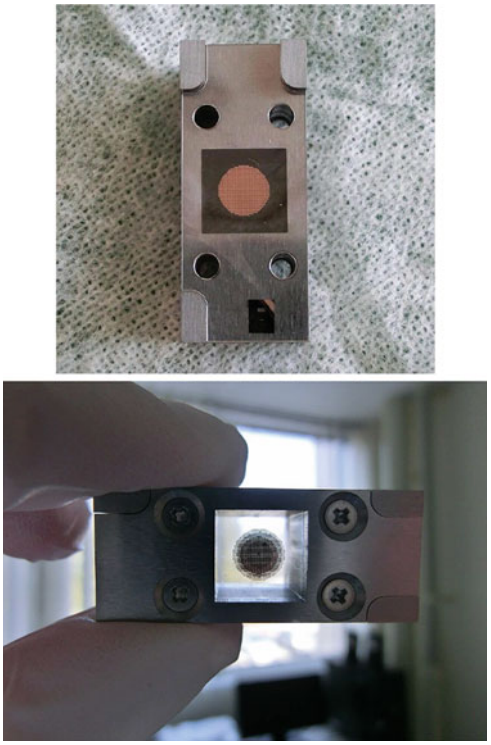

Fig. 12 Artificial dielectric lens with metal rectangular chips for terahertz wave band

4.23 mm at both 0.63 and 0.30 THz. The focus distance for 0.63 THz is shorter than that for 0.30 THz. These phenomena are also confirmed by the full wave analysis results shown in Fig. 5. The discrepancy of the local maximum values between the measurement and analysis may be the result of fabrication errors as well as deflection and chrome residues on the cyclo olefin polymer. The trends between the simulation and measurement results can be compared. The fabrication error and deflection are due to the fabrication of the lens base using a three-dimensional printer, which can fabricate the lens base relatively easily.

5.2 Measurement result for lens without buffer layer

Figure 12 shows the artificial dielectric lens with metal rectangular chips without the chrome buffer layer. The fabrication error of this lens's base is less than a few microns. The lenses were stacked manually and the air gap is about 12 μm. Figure 13 shows the measurement result for 0.48 THz and Fig. 14 shows those for 0.30 THz. The measurements are again performed using terahertz near-field microscopy, and the amplitude is expressed in dB. The focusing effect increases from 5.0 to 10.0 mm at both 0.48 and 0.30 THz. The trends between the simulation and measurement results can be compared. The terahertz wave is seen to focus along a line at 0.30 THz.

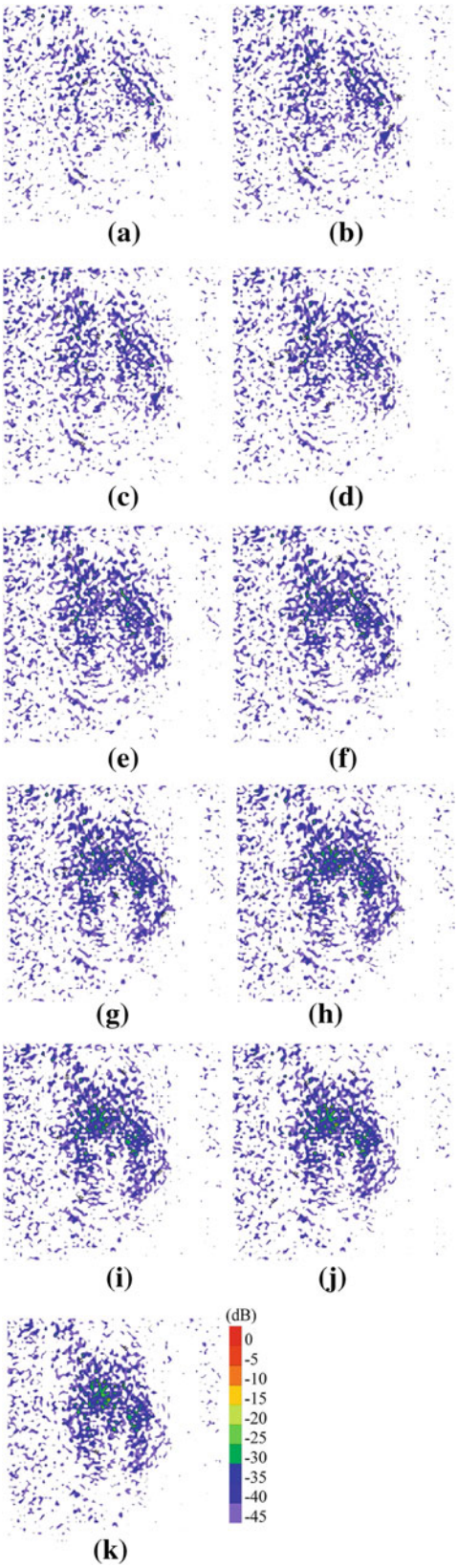

Fig. 13 Measurement results for aperture distribution of electric field through lens without buffer layer at 0.48 THz. (**a**) 5.0, (**b**) 5.5, (**c**) 6.0, (**d**) 6.5, (**e**) 7.0, (**f**) 7.5, (**g**) 8.0, (**h**) 8.5, (**i**) 9.0, (**j**) 9.5 and (**k**) 10.0 mm

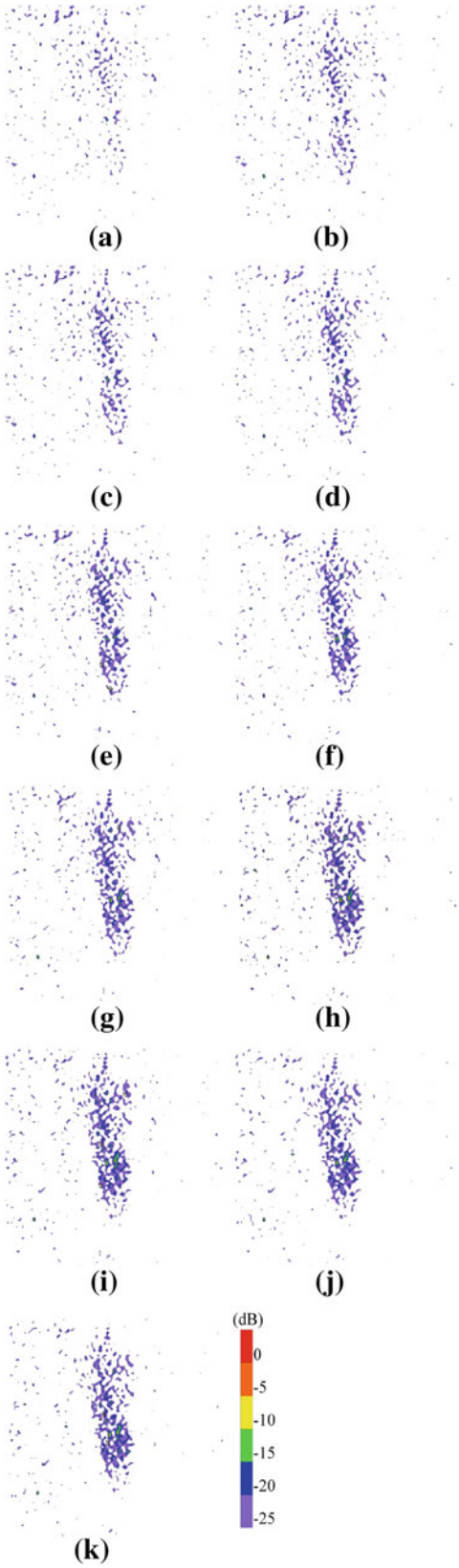

Fig. 14 Measurement results for aperture distribution of electric field through lens without buffer layer at 0.30 THz. (**a**) 5.0, (**b**) 5.5, (**c**) 6.0, (**d**) 6.5, (**e**) 7.0, (**f**) 7.5, (**g**) 8.0, (**h**) 8.5, (**i**) 9.0, (**j**) 9.5 and (**k**) 10.0 mm

6 Conclusions

We designed and fabricated artificial dielectric lenses with metal rectangular chips on a cyclo olefin polymer for the terahertz wave band. Two types of lenses were fabricated. The focusing effect was measured using terahertz near-field microscopy. The lens fabricated by laser processing has a chrome buffer layers which causes conductivity loss. The discrepancy between the measurement and analysis is primarily due to fabrication error and deflection from the three-dimensional printer. The lens fabricated by semiconductor etching does not have the buffer layer.

Acknowledgments The authors wish to thank Mr. A. Kuroda, Mr. W. Kurosaki, Prof. Y. Tomota for their assistance in the measurements. This research was partially supported by a Grant-in-Aid for Scientific Research on Innovative Areas "Electromagnetic Metamaterial" (No. 23109505) from the Ministry of Education, Culture, Sports, Science and Technology (MEXT), Japan, the Strategic Information and Communications R&D Promotion Programme (SCOPE) (No. 122103011) from the Ministry of Internal Affairs and Communications, Accelerating Utilization of University IP Program (No. 439) from Japan Science and Technology Agency (JST), Program for Revitalization Promotion (No. 241FT0462) from Japan Science and Technology Agency (JST), the Takayanagi Memorial Foundation, the Yazaki Memorial Foundation for Science & Technology, the Iketani Science and Technology Foundation, Futaba Electronics Memorial Foundation, and MEXT Nanotechnology platform 12025014(F-12-IT-0007).

References

1. W.E. Kock, Metallic delay lenses. Bell Syst. Tech. J. **27**(1), 58–82 (1948)
2. S.S.D. Jones, J. Brown, Metallic delay lenses. Nature **163**, 324–325 (1949)
3. J. Brown, The design of metallic delay dielectrics. Proc. Inst. Electr. Eng. Part 3 Radio Commun. Eng. **97**(45), 45–48 (1950)
4. S.B. Cohn, Microwave measurements on metallic delay media. Proc. IRE **41**(9), 1177–1183 (1953)
5. J. Brown, W. Jackson, The relative permittivity of tetragonal arrays of perfectly conducting thin discs. Proc. Inst. Electr. Eng. Part 3 Radio Commun. Eng. **102**(1), 37–42 (1955)
6. N.I. Landy, S. Sajuyigbe, J.J. Mock, D.R. Smith, W.J. Padilla, Perfect metamaterial absorber. Phys. Rev. Lett. **100**, 207402 (2008)
7. H. Tao, N.I. Landy, C.M. Bingham, X. Zhang, R.D. Averitt, W.J. Padilla, A metamaterial absorber for the terahertz regime: design, fabrication and characterization. Opt. Express **16**(10), 7181–7188 (2008)
8. H. Tao, C.M. Bingham, A.C. Strikwerda, D. Pilon, D. Shrekenhamer, N.I. Landy, K. Fan, X. Zhang, W.J. Padilla, R.D. Averitt, Highly flexible wide angle of incidence terahertz metamaterial absorber: design, fabrication, and characterization. Phys. Rev. B **78**, 241103 (2008)
9. N.I. Landy, C.M. Bingham, T. Tyler, N. Jokerst, D.R. Smith, W.J. Padilla, Design, theory, and measurement of a polarization-insensitive absorber for terahertz imaging. Phys. Rev. B **79**, 125104 (2009)
10. H.-T. Chen, J. Zhou, J.F. O'Hara, F. Chen, A.K. Azad, A.J. Taylor, Antireflection coating using metamaterials and identification of its mechanism. Phys. Rev. Lett. **105**, 073901 (2010)

11. M. Choi, S.H. Lee, Y. Kim, S.B. Kang, J. Shin, M.H. Kwak, K.-Y. Kang, Y.-H. Lee, N. Park, B. Min, A terahertz metamaterial with unnaturally high refractive index. Nature **470**, 369–374 (2011)
12. O. Paul, B. Reinhard, B. Krolla, R. Beigang, M. Rahm, Gradient index metamaterial based on slot elements. Appl. Phys. Lett. **96**, 241110 (2010)
13. J. Neu, B. Krolla, O. Paul, B. Reinhard, R. Beigang, M. Rahm, Metamaterial-based gradient index lens with strong focusing in the THz frequency range. Opt. Express **18**(26), 27748–27757 (2010)
14. A. Siemion, A. Siemion, M. Makowski, J. Suszek, J. Bomba, A. Czerwinski, F. Garet, J.L. Coutaz, M. Sypek, Diffractive paper lens for terahertz optics. Opt. Lett. **37**, 4320 (2012)
15. J. Lee, K. Lee, H. Park, G. Kang, D.H. Yu, K. Kim, Tunable subwavelength focusing with dispersion-engineered metamaterials in the terahertz regime. Opt. Lett. **35**, 2254 (2010)
16. V. Torres, V. Pancheco-Pena, P. Rodriguez-Ulibarri, M. Navarro-Cia, M. Beruete, M. Sorolla, N. Engheta, Terahertz epsilon-near-zero graded-index lens. Opt. Express **21**(7), 9156–9166 (2013)
17. T. Suzuki, T. Suzuki, J.C. Young, K. Takano, H. Kitahara, M. Hangyo, Analysis of artificial dielectric lens with metallic rectangular chips for terahertz wave band. Appl. Phys. A **109**(4), 825–830 (2012)
18. F. Miyamaru, M.W. Takeda, K. Taima, Characterization of terahertz metamaterials fabricated on flexible plastic films: toward fabrication of bulk metamaterials in terahertz region. Appl. Phys. Express **2**, 042001 (2009)
19. F. Miyamaru, S. Kubota, K. Taima, K. Takano, M. Hangyo, M.W. Takeda, Three-dimensional bulk metamaterials operating in the terahertz range. Appl. Phys. Lett. **96**, 081105 (2010)
20. IEICE, *Antenna Engineering Handbook*, 2nd edn. (Ohmsha, Tokyo, 2008) Sect. 6.4.3
21. H. Kitahara, Y. Yakiyama, K. Takano M. Hangyo, Imaging of the metamaterials using terahertz near-field microscopy. International Symposium on Frontier in THz Technology 2012, Pos2.9 (2012)
22. C.A. Balanis, *Antenna theory: analysis and design*, 3rd edn. (Wiley, New York, 2005). Sect. 4.7.1